NASA TECHNICAL NOTE

NASA TN D-6759

PITOT-PROBE DISPLACEMENT IN A SUPERSONIC TURBULENT BOUNDARY LAYER

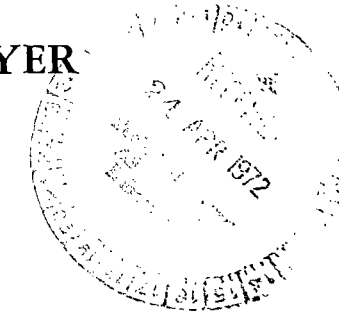

by Jerry M. Allen

Langley Research Center
Hampton, Va. 23365

NATIONAL AERONAUTICS AND SPACE ADMINISTRATION • WASHINGTON, D. C. • APRIL 1972

1. Report No.	2. Government Accession No.	3. Recipient's Catalog No.
NASA TN D-6759		

4. Title and Subtitle

PITOT-PROBE DISPLACEMENT IN A SUPERSONIC TURBULENT BOUNDARY LAYER

5. Report Date: April 1972

6. Performing Organization Code:

7. Author(s)

Jerry M. Allen

8. Performing Organization Report No.: L-8159

9. Performing Organization Name and Address

NASA Langley Research Center
Hampton, Va. 23365

10. Work Unit No.: 760-74-01-04

11. Contract or Grant No.:

12. Sponsoring Agency Name and Address

National Aeronautics and Space Administration
Washington, D.C. 20546

13. Type of Report and Period Covered: Technical Note

14. Sponsoring Agency Code:

15. Supplementary Notes

16. Abstract

Eight circular pitot probes ranging in size from 2 to 70 percent of the boundary-layer thickness have been tested to provide experimental probe displacement results in a two-dimensional turbulent boundary layer at a nominal free-stream Mach number of 2 and unit Reynolds number of 8×10^6 per meter. The displacement obtained in this study was larger than that reported by previous investigators in either an incompressible turbulent boundary layer or a supersonic laminar boundary layer.

The large probes indicated distorted Mach number profiles, probably due to separation. When the probes were small enough to cause no appreciable distortion, the displacement was constant over most of the boundary layer. The displacement in the near-wall region decreased to negative displacement in some cases. This near-wall region was found to extend to about one probe diameter from the test surface.

17. Key Words (Suggested by Author(s))	18. Distribution Statement
Turbulent boundary layer Pitot-probe displacement Supersonic	Unclassified – Unlimited

19. Security Classif. (of this report)	20. Security Classif. (of this page)	21. No. of Pages	22. Price*
Unclassified	Unclassified	29	$3.00

*For sale by the National Technical Information Service, Springfield, Virginia 22151

PITOT-PROBE DISPLACEMENT IN A SUPERSONIC TURBULENT BOUNDARY LAYER

By Jerry M. Allen
Langley Research Center

SUMMARY

Eight circular pitot probes ranging in size from 2 to 70 percent of the boundary-layer thickness have been tested to provide experimental probe displacement results in a two-dimensional turbulent boundary layer at a nominal free-stream Mach number of 2 and unit Reynolds number of 8×10^6 per meter. The displacement obtained in this study was larger than that reported by previous investigators in either an incompressible turbulent boundary layer or a supersonic laminar boundary layer.

The large probes indicated distorted Mach number profiles, probably due to separation. When the probes were small enough to cause no appreciable distortion, the displacement was constant over most of the boundary layer. The displacement in the near-wall region decreased to negative displacement in some cases. This near-wall region was found to extend to about one probe diameter from the test surface.

INTRODUCTION

It has long been known that a pitot probe placed in incompressible shear flow does not measure the true pressure that exists at the center of the probe in the undisturbed stream. Three factors are known to contribute to these erroneous measurements: (1) the streamlines of the undisturbed flow being deflected because of the physical presence of the probe in the shear gradient, (2) the average pressure across the face of the probe, which is presumably what the probe should measure, not being the same as the pressure at the geometric center of the orifice, and (3) viscosity effects on the probe readings. This last factor occurs only when the local Reynolds number based on probe diameter is very small (ref. 1) and thus can be neglected in most practical cases. Because of factors (1) and (2), therefore, the pressure measured by a pitot probe in incompressible shear flow is not the pressure at the geometric center of the probe in undisturbed flow. The effective center is thus said to be "displaced" from the geometric center. Corrections to pitot-probe measurements can be made for this effect, however, if the magnitude and direction of the displacement are known. In supersonic flow, the bow shock wave wrapped around the probe provides an additional complication to the flow pattern.

Previous theoretical studies on probe displacement can be divided into those which investigate the first factor, streamline deflection, and those which investigate the second, average pressure. The studies of Hall (ref. 2) and Lighthill (ref. 3) fall into the first category and agree that the probe displacement in free shear flow should be in the direction of higher velocity, hereafter referred to as positive displacement.

The works of Hsu (ref. 4) and Fenter and Stalmach (ref. 5) fall into the second category. Using the incompressible law of the wall, Hsu calculates the theoretical pressure distribution across the face of a circular pitot probe in contact with the test surface. The integration of this pressure distribution then reveals that the average pressure felt by the probe should be lower than the pressure at the center of the probe, that is, negative displacement. Similar results were obtained by Fenter and Stalmach using the compressible law of the wall.

Notice that the streamline-deflection studies and the average-pressure studies give opposite trends. It might be hypothesized that in free shear flow or in the outer part of a boundary layer, the streamline-deflection factor would dominate; whereas in the lower part of a boundary layer, where the law of the wall is valid and where the proximity of the wall limits streamline deflection, the average-pressure factor would dominate. In any event, the combined effect of these or any other factors could be determined by experimental investigation.

Previous experimental studies on probe displacement can be divided into three general categories: those conducted in free shear flow, those in laminar boundary layers, and those in turbulent boundary layers or pipe flow. For clarity, the following table is used to summarize the general results of previous studies in these three categories:[a]

Reference	Investigator	Probe shape	D/δ	Mach number	Reynolds number, per meter	General results
			Free shear flow (wakes)			
6	Young and Maas	Circular	0.02 to 0.27	0	1.3×10^6	$\Delta/D \approx 0.18$
7	Johannesen and Mair	Circular	0.3 to 6.0	1.96	13.0×10^6	No displacement
8	Marson and Lilley	Circular	0.62 to 14.2	0 to 3.2	1.0 to 13.7×10^6	$\Delta/D \approx 0.18$, but decreasing for large D
9	P. Davies	Circular	0.01 to 3.2	0	1.5×10^6	Positive displacement
10	Sami	Circular	<0.04	0	0.6 to 1.1×10^6	Positive displacement
			Laminar boundary layers			
11	F. Davies	Circular	0.18 to 1.18	2.30	10.0 to 12.0×10^6	$\Delta/D \approx -0.15$
12	Blue and Low	Rectangular	0.06 to 0.32	2 and 3	5.0 to 9.9×10^6	Negative displacement
			Turbulent boundary layers or pipe flow			
11, 13	Cole and Cope	Circular	0.08	2.5	3.3×10^6	Positive displacement near wall
11, 13	Cole and Cope	Rectangular	0.02 to 0.16	2.5	3.3×10^6	Negative displacement for probes touching wall
14	Preston	Circular	0.03 to 0.12	0	0.6 to 2.4×10^6	$0.12 < \Delta/D < 0.18$ for probes touching wall
14	Preston	Rectangular	0.003	0	3.0×10^6	Negative displacement near wall
15	MacMillan	Circular	0.02 to 0.12	0	0.5 to 2.3×10^6	$\Delta/D \approx 0.15$, but decreases near wall
16	Livesey	Circular	0.01 to 0.13	0	0.5×10^6	$\Delta/D \approx 0.09$
9	P. Davies	Circular	0.04 to 0.69	0	1.5×10^6	No displacement
17	Quarmby and Das	Rectangular	0.02 to 0.09	0	0.6 to 1.3×10^6	$\Delta/D \approx 0.19$, but decreases near wall

[a] The following symbols are used in the table:

D	external diameter of circular pitot probe or external height of rectangular pitot probe
δ	boundary-layer thickness
Δ	pitot-probe displacement

One of the primary areas of interest in fluid mechanics is the compressible turbulent boundary layer. The table shows that there is a scarcity of experimental data on probe displacement under these conditions. One paper, Cole and Cope (ref. 13), does contain a small amount of data in this area, but only as an incidental part of the primary subject.

The comprehensive study of MacMillan (ref. 15) in an incompressible turbulent boundary layer shows that the displacement is positive in the outer part of the boundary layer and decreases somewhat as the wall is approached but still remains positive. This result tends to support the relative importance of factors (1) and (2) discussed earlier. Whether the existence of the bow shock in front of the pitot probe in a supersonic boundary layer alters this displacement pattern is unknown because of the lack of experimental data in this region. Hence, the present study was performed to provide experimental data on pitot-probe displacement in a supersonic turbulent boundary layer.

SYMBOLS

U.S. Customary Units were employed for the measurements, but the International System of Units (SI) is used to report the results.

d	internal diameter of circular pitot probe
D	external diameter of circular pitot probe or external height of rectangular pitot probe
M	Mach number
N	exponent in velocity-profile power law, $\frac{u}{u_e} \propto y^{1/N}$
p	static pressure
p_t'	measured total (pitot) pressure
R_D	Reynolds number based on D, $\frac{\rho_e u_e D}{\mu_e}$
T	temperature
u	local velocity

y	normal coordinate
δ	total boundary-layer thickness (6.99 cm in this paper)
δ^*	boundary-layer displacement thickness (see eq. (8))
Δ	pitot-probe displacement
θ	boundary-layer momentum thickness (see eq. (7))
μ	viscosity
γ	ratio of specific heats
ρ	density

Subscripts:

e	boundary-layer edge
max	maximum value
o	evaluated at $D = 0$
t	stagnation

APPARATUS AND TESTS

Wind Tunnel

The investigation was conducted in the Langley 4- by 4-foot supersonic pressure tunnel, which is described in reference 18. This facility is a rectangular, closed-test-section, single-return wind tunnel with provisions for control of pressure, temperature, and humidity of the enclosed air. Two flexible walls of the two-dimensional nozzle can be adjusted to give Mach numbers from 1.4 to 2.6. The maximum operating stagnation pressure is about 2 atm (1 atm = 1.013×10^5 N/m^2), and the normal operating stagnation temperature is about 43° C.

Test Station

The tunnel sidewall was used as the model in this investigation. The boundary layer on the sidewall was surveyed on the wall center line at a station in the downstream part

of the test section to provide for a long run of turbulent flow and a thick boundary layer. The survey station was located about 5 meters from the nozzle throat, providing a turbulent boundary layer about 7 cm thick. The permanent model support mechanism was located downstream of the survey station and was traversed to the opposite side of the test section to insure that no flow disturbances originating from the mechanism could affect the data taken during this test. Test-section static pressure was measured at orifices on the tunnel sidewall about 1.6 meters upstream of the test station. Figure 1 is a sketch of the general test setup.

Instrumentation

The tunnel sidewall boundary layer was surveyed with nine pitot probes ranging in size from 0.26 mm to 48 mm (2 to 70 percent of the boundary-layer thickness). The smallest probe was a conventional flattened boundary-layer probe and was used to provide a reference survey of the boundary layer. The remaining eight probes were circular, with ratios of inside diameter to outside diameter of about 0.6. These probes were used to obtain the displacement data. Sketches of the probes can be found in figure 2.

Small-diameter tubing was used between the pressure-measuring transducer and the downstream end of the pitot-tube bore (fig. 2). For the largest pitot probe tested, measurements obtained by use of this arrangement were essentially the same as check measurements obtained by relocating the pitot-tube bore outlet about 180° from the location shown in figure 2.

The probes were mounted on a shaft which ran through the tunnel sidewall. An O-ring seal was used between the shaft and the sidewall to eliminate leakage. Probe position normal to the wall was controlled manually from outside the tunnel by a traversing mechanism connected to the probe shaft. The surface location was determined by electrical contact between the wall and the probe tip, and the position above the test surface was determined from the surface contact point and a dial indicator connected to the probe shaft.

Pitot-probe pressures were measured by a pressure transducer having a range of 0 to 0.69 atm and a nominal accuracy of about 0.25 percent of its full-scale reading. Tunnel stagnation and test-section static pressures were measured by precision automatic indicating mercury manometers. All data were recorded on magnetic tape for data reduction purposes.

Tests and Procedures

The test was conducted at a nominal free-stream Mach number of 2 and a stagnation pressure of 0.69 atm. Tunnel stagnation temperature was maintained at about 41° C so that the wall temperature would be very close to ambient temperature outside the test

section. This insured that no appreciable temperature gradient was present across the tunnel wall, hence the test was run near zero heat-transfer conditions.

The above test conditions result in a free-stream unit Reynolds number of about 8×10^6 per meter and a Reynolds number based on the distance from the tunnel throat to the survey station of about 43×10^6. The tunnel dewpoint was maintained at about -29° C.

The boundary layer at the test station was surveyed by each of the probes in turn. The test procedure consisted of bringing the probe in contact with the tunnel wall, as determined by the contact light, and then moving the probe away from the wall in small increments, and recording data. The increments were adjusted so that each probe had its center at identical positions across the boundary layer. A complete boundary-layer survey by each probe took about 20 minutes.

DATA REDUCTION

The measured wall static pressure p was assumed to be constant throughout the test section and was combined with the measured values of pitot pressure p_t' to form the ratio p_t'/p from which the local Mach number of each data point was calculated. The subsonic Mach numbers $(p_t'/p$ less than $1.893)$ were calculated from the isentropic equation

$$\frac{p_t'}{p} = \left(1 + \frac{\gamma - 1}{2} M^2\right)^{\frac{\gamma}{\gamma-1}} \tag{1}$$

The supersonic Mach numbers $(p_t'/p$ greater than $1.893)$ were calculated from the Rayleigh pitot formula

$$\frac{p_t'}{p} = \left(\frac{\gamma + 1}{2} M^2\right)^{\frac{\gamma}{\gamma-1}} \left(\frac{\gamma + 1}{2\gamma M^2 - \gamma + 1}\right)^{\frac{1}{\gamma-1}} \tag{2}$$

The Mach number at the boundary-layer edge was selected by inspection to be 1.975, which is about 1 percent lower than the nominal free-stream value of 2. Previous calibrations of this tunnel had shown a slight reduction in free-stream Mach number close to the tunnel sidewalls; therefore, this Mach number difference was not unexpected and is not due to measurement inaccuracies. Free-stream Mach numbers calculated from test-section static and settling-chamber stagnation pressures were very close to the nominal Mach number.

Velocity ratios were calculated from

$$\frac{u}{u_e} = \frac{M}{M_e}\sqrt{\frac{T}{T_t}}\sqrt{\frac{T_{t,e}}{T_e}}\sqrt{\frac{T_t}{T_{t,e}}} \tag{3}$$

where

$$\frac{T_t}{T} = 1 + \frac{\gamma - 1}{2} M^2$$

and

$$\frac{T_{t,e}}{T_e} = 1 + \frac{\gamma - 1}{2} M_e^2 \tag{4}$$

The total temperature distribution across the boundary layer was assumed to be constant and equal to $T_{t,e}$. This assumption has been shown by previous investigators to have a negligible effect on the experimental integral thicknesses for the flow conditions in this paper. (See refs. 12 and 19, for example.) The velocity ratios can therefore be written as

$$\frac{u}{u_e} = \frac{M}{M_e}\sqrt{\frac{1 + \frac{\gamma - 1}{2} M_e^2}{1 + \frac{\gamma - 1}{2} M^2}} \tag{5}$$

If static pressure and total temperature are assumed to be constant across the boundary layer, the density ratio can be written as

$$\frac{\rho}{\rho_e} = \frac{T_e}{T} = \frac{1 + \frac{\gamma - 1}{2} M^2}{1 + \frac{\gamma - 1}{2} M_e^2} \tag{6}$$

Experimental values of momentum thickness θ and displacement thickness δ^* were calculated from the two-dimensional compressible flow equations

$$\theta = \int_0^{\delta} \frac{\rho u}{\rho_e u_e}\left(1 - \frac{u}{u_e}\right) dy \tag{7}$$

and

$$\delta^* = \int_0^{\delta} \left(1 - \frac{\rho u}{\rho_e u_e}\right) dy \tag{8}$$

Equations (5) and (6) allow the calculation of the integrands in equations (7) and (8) for each data point in the boundary layer. The integrations were performed by parabolic-curve fitting through successive data points and stepwise integration of the resulting curves.

RESULTS AND DISCUSSION

Probe Size Effects

Probe displacement effects were evaluated in terms of the Mach number values measured by these probes, as can be seen in figure 3 where the probe Mach numbers are plotted as a function of probe diameter. The curves connect points of constant y/δ, that is, points whose probe centers are located at the same position in the boundary layer. The extrapolation of these curves to $D = 0$ should give the true Mach number profile for this boundary layer. The solid symbols indicate points where the probes were touching the wall.

At the smaller diameters there appears to be a linear increase in indicated Mach number with probe diameter. Straight lines were thus faired through the small-diameter points to get the $D = 0$ points. The indicated Mach number being larger than the true Mach number is termed "positive displacement."

Proceeding from left to right along any one curve in this figure results in the probe coming into closer proximity to the wall, since the centers of the probes remain at the same location and the diameters increase. This wall influence region causes the displacement to decrease at the larger probe diameters. The point at which deviation from the linear curve begins is about one probe diameter from the wall. Note that the Mach numbers measured at the wall contact points (solid symbols) are close to the true Mach number at that value of y/δ. This result indicates that probe displacement effects in Preston tube work are probably negligible.

The kinks in the curves in the upper right of this figure result from distortion of the boundary layer by the larger probes. Note that some of the indicated Mach numbers are larger than the value at the boundary-layer edge, referred to hereafter as Mach number overshoot. The gross distortion patterns seen here are probably caused by separation of the boundary layer upstream of the large probes. This separation would violate the normal-shock assumption in the data reduction equations and would hence lead to erro-

neously large indicated Mach numbers. The data for y/δ values larger than 0.782 were omitted from this figure for clarity, since these curves would simply fair into the dotted line as the boundary-layer edge is approached.

Mach Number Profiles

The true Mach number profile, obtained from the intersection of the curves in figure 3 with $D = 0$, is compared in figure 4 with the profile obtained from the flattened reference probe, which is the type normally used in boundary-layer research. The results from this type of probe generally do not require displacement corrections, since the probe dimension in the direction of the velocity gradient is small. The good agreement shown in this figure between the extrapolated profile and the flattened-probe profile indicates that the linear extrapolation was reasonable and that this is the true profile for this boundary layer.

This true profile is further examined in log-log form in figure 5, where it is seen to be a normal turbulent-boundary-layer velocity profile which follows a power-law exponent N of about 6.7. The boundary-layer thickness δ was estimated from this profile by the method developed in reference 20. In this method, the profile is plotted in the manner shown in figure 6. The straight-line fit to the data in the outer part of the boundary layer is extrapolated to $\frac{u}{u_e} = 1$ $\left(\text{or } \sqrt{1 - \frac{u}{u_e}} = 0\right)$. This point of intersection is defined as the boundary-layer thickness. Figure 6 shows this point to be at a value of $y^{1.5}$ of about 18.5 $cm^{1.5}$, which yields the boundary-layer thickness of this profile to be 6.99 cm.

The displacement effect of these probes can be seen by comparing the indicated profiles with the true profile, as shown in figure 7. The profiles from the two smallest probes appear normal in shape while showing small positive displacement over most of the boundary layer. The $\frac{D}{\delta} = 0.145$ profile contains a small region of distortion near the wall. This region spreads and becomes more pronounced with increasing probe size. Profiles from the two largest probes have the regions of Mach number overshoot mentioned previously. These Mach numbers from the eight circular probes and the flattened reference probe, along with the true profile, are listed in table I.

This overshoot phenomenon has been noticed by other investigators, who have used large probes in supersonic flow. (See, for example, references 7 and 8 for supersonic wake results and reference 11 for supersonic laminar-boundary-layer results.)

Figure 8 shows a comparison of the turbulent overshoot results of this study with the laminar results of reference 11 at comparable Mach numbers. The laminar overshoot is avoided if the probe diameter is less than about 20 percent of the boundary-layer thickness, whereas the turbulent overshoot is not present until the probe is about 40 percent of the boundary-layer thickness. It should be noted from figure 7, however, that sig-

nificant distortion within the boundary layer occurs at probe sizes as small as 15 percent of the boundary-layer thickness. This distortion does not appear as overshoot, however, until the larger probe diameters.

Integral Thicknesses

The integration of the profiles in table I yielded the experimental momentum and displacement thicknesses, which are listed in table II. The true momentum thickness of this boundary layer is about 4.8 mm; thus, the present study was conducted at a Reynolds number based on momentum thickness of about 3.6×10^4.

The influence of probe size on the integral thicknesses is shown in figure 9. This figure reveals a substantial effect resulting from probe displacement and distortion, which increases with probe size. The integral thicknesses obtained from the flattened reference probe are within 1 percent of the true values.

Displacement Distributions

As the name implies, the displacement effect of these probes is the distance that the measured data is displaced from the true profile, which in figure 7 is simply the horizontal distances between the symbols and the curve. These displacement distances were measured for each data point on this figure and are shown in figure 10. For the smaller probes, the displacement appears, within the accuracy of the data, to be constant over most of the boundary layer. For small y/δ values, it decreases to near zero because of the wall effect mentioned previously. The relatively large scatter in the data near the boundary-layer edge is caused by the small Mach number gradients in this region, and therefore accurate displacement measurements were difficult to obtain. The displacement distributions were thus faired to zero at $\frac{y}{\delta} = 1$, since there is no probe displacement effect in the gradient-free free stream.

The distortion regions, which begin with the $\frac{D}{\delta} = 0.145$ profile, appear as peaks in the displacement curves. Above these distortion regions, however, there are still regions for the moderate diameter probes $\left(\frac{D}{\delta} = 0.145, 0.255, \text{ and } 0.364\right)$ where the displacement remains constant before dropping to zero in the free stream. For the $\frac{D}{\delta} = 0.473$ probe, the distortion covers most of the boundary layer; therefore, there is no room for the constant-displacement region. The two largest probes, which contain the regions of Mach number overshoot, show regions of indeterminate displacement because of the definition of displacement presented previously.

Displacement Ratios

Previous experiments in incompressible flow have shown that the ratio of displacement to probe diameter is independent of probe diameter in the absence of wall effects.

Hence the constant-level values of displacement were divided by the respective probe diameter and are shown in figure 11 as a function of probe diameter. The point at $D = 0$ in this figure was not measured in the manner described previously but was estimated from the slopes of the lines in figure 3 ($\partial M/\partial D$) and the slopes of the true Mach number profile ($\partial M/\partial y$) in the following manner: By definition, the value of $\frac{M - M_o}{y - y_o}$ approaches $\partial M/\partial y$ as D approaches zero. But $y - y_o$ is simply the displacement Δ, and $M - M_o$ can be seen in figure 3 to be equal to $D \frac{\partial M}{\partial D}$ for small D because of the linearity assumption. Therefore, in the limiting case of vanishingly small D,

$$\frac{\frac{\partial M}{\partial D} D}{\Delta} = \frac{\partial M}{\partial y}$$

or

$$\frac{\Delta}{D} = \frac{\partial M/\partial D}{\partial M/\partial y}$$

at $D = 0$.

Values of Δ/D were calculated from this equation for each y value for which data were available and are shown in figure 12. The ratio remains relatively constant over the boundary layer and yields an average value of about 0.38. This is the value shown at $D = 0$ in figure 11 and is the value that Δ/D should approach for small values of D. It can be seen that this limiting value agrees well with those from the smaller probes. The larger probes, however, show decreasing values in the constant-displacement regions. It is interesting to note that if the maximum values of Δ/D are plotted instead of the constant-displacement values, the agreement with the smaller probe data is good.

Included in figure 11 for comparison are the levels of Δ/D obtained by previous investigators in an incompressible turbulent boundary layer (ref. 15) and a supersonic laminar boundary layer (ref. 11). For small values of D/δ, which is the range of most practical interest in boundary-layer research, the present results (supersonic, turbulent) are more than twice as large as those of reference 15 (incompressible, turbulent). The supersonic laminar results of reference 11, on the other hand, show a negative displacement of about the same magnitude as the incompressible turbulent results.

It is interesting to compare the displacement ratios from the probes resting on the test surface with those which Preston (ref. 14) obtained in incompressible pipe flow. Figure 13 shows these ratios as a function of the Reynolds number parameter used by Preston. It can be seen that the trends of the two sets of data are not similar and that the displace-

ment of the supersonic data is, generally, much smaller than that of the incompressible data. When these results are compared with the displacement levels shown in figure 11, it can be seen that the incompressible results of probes resting against the test surface are of the same order of magnitude as those from probes farther out in the boundary layer. The supersonic results, on the other hand, are generally an order of magnitude less.

CONCLUSIONS

Eight circular pitot probes ranging in size from 2 to 70 percent of the boundary-layer thickness have been tested to provide experimental probe displacement results in a two-dimensional supersonic turbulent boundary layer. The primary conclusions to be drawn from this study are:

1. Pitot-probe displacement obtained in this study is larger than that obtained by previous investigators in either an incompressible turbulent boundary layer or a supersonic laminar boundary layer.

2. The proximity of the wall tends to reduce the displacement effect in the near-wall region and, in some cases, to cause negative displacement.

3. This near-wall region extends to about one probe diameter from the test surface.

4. Although all probes show displacement effects, only the large probes distort the shape of the indicated boundary-layer profile.

5. When probes are small enough to cause no distortion, the displacement is constant over most of the boundary layer.

Langley Research Center,
National Aeronautics and Space Administration,
Hampton, Va., March 10, 1972.

REFERENCES

1. Kane, E. D.; and Maslach, G. J.: Impact-Pressure Interpretation in a Rarefied Gas at Supersonic Speeds. NACA TN 2210, 1950.

2. Hall, I. M.: The Displacement Effect of a Sphere in a Two-Dimensional Shear Flow. J. Fluid Mech., vol. 1, pt. 2, July 1956, pp. 142-162.

3. Lighthill, M. J.: Contributions to the Theory of the Pitot-Tube Displacement Effect. J. Fluid Mech., vol. 2, pt. 5, July 1957, pp. 493-512.

4. Hsu, E. Y.: The Measurement of Local Turbulent Skin Friction by Means of Surface Pitot Tubes. Rep. 957, David W. Taylor Model Basin, Navy Dept., Aug. 1955.

5. Fenter, Felix W.; and Stalmach, Charles J., Jr.: The Measurement of Local Turbulent Skin Friction at Supersonic Speeds by Means of Surface Impact Pressure Probes. DRL-392, CM-878 (Contract NOrd-16498), Univ. of Texas, Oct. 21, 1957.

6. Young, A. D.; and Maas, J. N.: The Behaviour of a Pitot Tube in a Transverse Total-Pressure Gradient. R. & M. No. 1770, Brit. A.R.C., 1937.

7. Johannesen, N. H.; and Mair, W. A.: Experiments With Large Pitot Tubes in a Narrow Supersonic Wake. J. Aeronaut. Sci., vol. 19, no. 11, Nov. 1952, pp. 785-787.

8. Marson, G. B.; and Lilley, G. M.: The Displacement Effect of Pitot Tubes in Narrow Wakes at Subsonic and Supersonic Speeds. Rep. No. 107, Coll. of Aeronaut., Cranfield (Engl.), Oct. 1956.

9. Davies, P. O. A. L.: The Behaviour of a Pitot Tube in Transverse Shear. J. Fluid Mech., vol. 3, pt. 5, Feb. 1958, pp. 441-456.

10. Sami, Sedat: The Pitot Tube in Turbulent Shear Flow. Developments in Mechanics, Vol. 5, H. J. Weiss, D. F. Young, W. F. Riley, and T. R. Rogge, eds., Iowa State Univ. Press, 1969, pp. 191-200.

11. Davies, F. V.: Some Effects of Pitot Size on the Measurement of Boundary Layers in Supersonic Flow. Tech. Note No. Aero. 2179, Brit. R.A.E., Aug. 1952.

12. Blue, Robert E.; and Low, George M.: Factors Affecting Laminar Boundary Layer Measurements in a Supersonic Stream. NACA TN 2891, 1953.

13. Cole, J. A.; and Cope, W. F.: Boundary Layer Measurements at a Mach Number of $2\frac{1}{2}$ in the Presence of Pressure Gradients. NPL Eng. Div. No. 420/49, Brit. A.R.C., May 1949.

14. Preston, J. H.: The Determination of Turbulent Skin Friction by Means of Pitot Tubes. J. Roy. Aeronaut. Soc., vol. 58, no. 518, Feb. 1954, pp. 109-121.

15. MacMillan, F. A.: Experiments on Pitot-Tubes in Shear Flow. R. & M. No. 3028, Brit. A.R.C., 1957.

16. Livesey, J. L.: Behavior of Transverse Cylindrical and Forward Facing Total Pressure Probes in Transverse Total Pressure Gradients. J. Aeronaut. Sci., vol. 23, no. 10, Oct. 1956, pp. 949-955.

17. Quarmby, Alan; and Das, H. K.: Displacement Effects on Pitot Tubes With Rectangular Mouths. Aeronaut. Quart., vol. XX, pt. 2, May 1969, pp. 129-139.

18. Schaefer, William T., Jr.: Characteristics of Major Active Wind Tunnels at the Langley Research Center. NASA TM X-1130, 1965.

19. Adcock, Jerry B.; Peterson, John B., Jr.; and McRee, Donald I.: Experimental Investigation of a Turbulent Boundary Layer at Mach 6, High Reynolds Numbers, and Zero Heat Transfer. NASA TN D-2907, 1965.

20. Peterson, John B., Jr.: Boundary-Layer Velocity Profiles Downstream of Three-Dimensional Transition Trips on a Flat Plate at Mach 3 and 4. NASA TN D-5523, 1969.

TABLE I.- MACH NUMBER PROFILES[a]

y/δ	Mach number for circular probes for D/δ of –								Mach number for –	
	0.018	0.034	0.145	0.255	0.364	0.473	0.582	0.691	Flattened reference probe	True profile
0.003	----------	----------	----------	----------	----------	----------	----------	----------	0.608, 0.611	----
.009	0.893, 0.889	----------	----------	----------	----------	----------	----------	----------	.901	----
.017	1.008	0.984, 0.983	----------	----------	----------	----------	----------	----------	.993	----
.073	1.243	1.252	1.254, 1.256	----------	----------	----------	----------	----------	1.239	1.229
.127	1.336	1.348	1.397	1.336, 1.338	----------	----------	----------	----------	1.337	1.329
.182	1.412	1.419	1.474	1.467	1.405, 1.406	----------	----------	----------	1.407	1.402
.236	1.466	1.475	1.537	1.550	1.518	1.460, 1.462	----------	----------	1.465	1.457
.291	1.525	1.534	1.578	1.618	1.608	1.569	1.506, 1.505	----------	1.522	1.518
.345	1.582	1.586	1.631	1.669, 1.665	1.686, 1.679	1.652	1.611	1.538, 1.545	1.576	1.574
.400	1.626	1.638	1.678	1.694, 1.710	1.749, 1.752	1.737	1.685	1.634	1.625	1.621
.455	1.681	1.686	1.730	1.738, 1.738	1.789, 1.792	1.807	1.767	1.722	1.672	1.674
.509	1.722	1.731	1.769	1.773	1.806, 1.818	1.871	1.840	1.797	1.721	1.715
.564	1.769	1.777	1.816	1.815	1.831, 1.835	1.898	1.914	1.865	1.766	1.760
.618	1.807	1.818	1.851	1.856	1.866	1.915	1.977	1.946	1.810	1.802
.673	1.855	1.860	1.882	1.888	1.902, 1.902	1.928	1.992	2.014	1.843	1.849
.727	1.882	1.890	1.909	1.920	1.924, 1.926	1.945	1.979	2.059	1.885	1.880
.782	1.917	1.925	1.940	1.941	1.942, 1.951	1.959	1.975	2.043	1.912	1.916
.836	1.935	1.947	1.958	1.953	1.955, 1.965	1.970	1.977	2.012	1.935	1.937
.891	1.952	1.962	1.969	1.963	1.966	1.979	1.979	2.002	1.959	1.955
.945	1.970	1.969	1.972	1.971	1.969	1.976	1.976	1.986	1.967	1.965
1.000	1.978	1.978	1.981	1.971	1.970	1.983	1.974	1.980	1.975	1.975
1.055	1.978	1.983	1.981	1.969	1.965	1.978	1.972	1.981	1.981	↓
1.109	1.974	1.984	1.981	1.979	1.966	1.979	1.974	1.981	1.978	
1.164	1.978	1.982	1.979	1.979	1.972	1.985	1.979	1.982	1.978	
1.218	1.976	1.982	1.983	1.972	1.972	1.984	1.979	1.985	1.978	
1.273	1.978	1.986	1.985	1.974	1.974	1.990	1.979	1.988	1.977	
1.327	1.982	1.987	1.985	1.984	1.977	1.990	1.980	1.983	1.983	
1.382	1.979	1.990	1.986	1.985	1.973	1.991	1.977	1.985	1.980	
1.436	1.981	1.989	1.985	1.981	1.973	1.984	1.980	1.983	1.984	

[a] When two values appear, the second is a repeat point.

TABLE II.- INTEGRAL THICKNESSES

D/δ	θ, mm	δ^*, mm
0.018	4.74	14.36
.034	4.59	14.13
.145	3.85	13.37
.255	3.49	13.90
.364	3.06	14.31
.473	2.59	14.68
.582	2.29	15.63
.691	2.01	16.56
Flattened reference probe	4.81	14.44
True profile	4.84	14.57

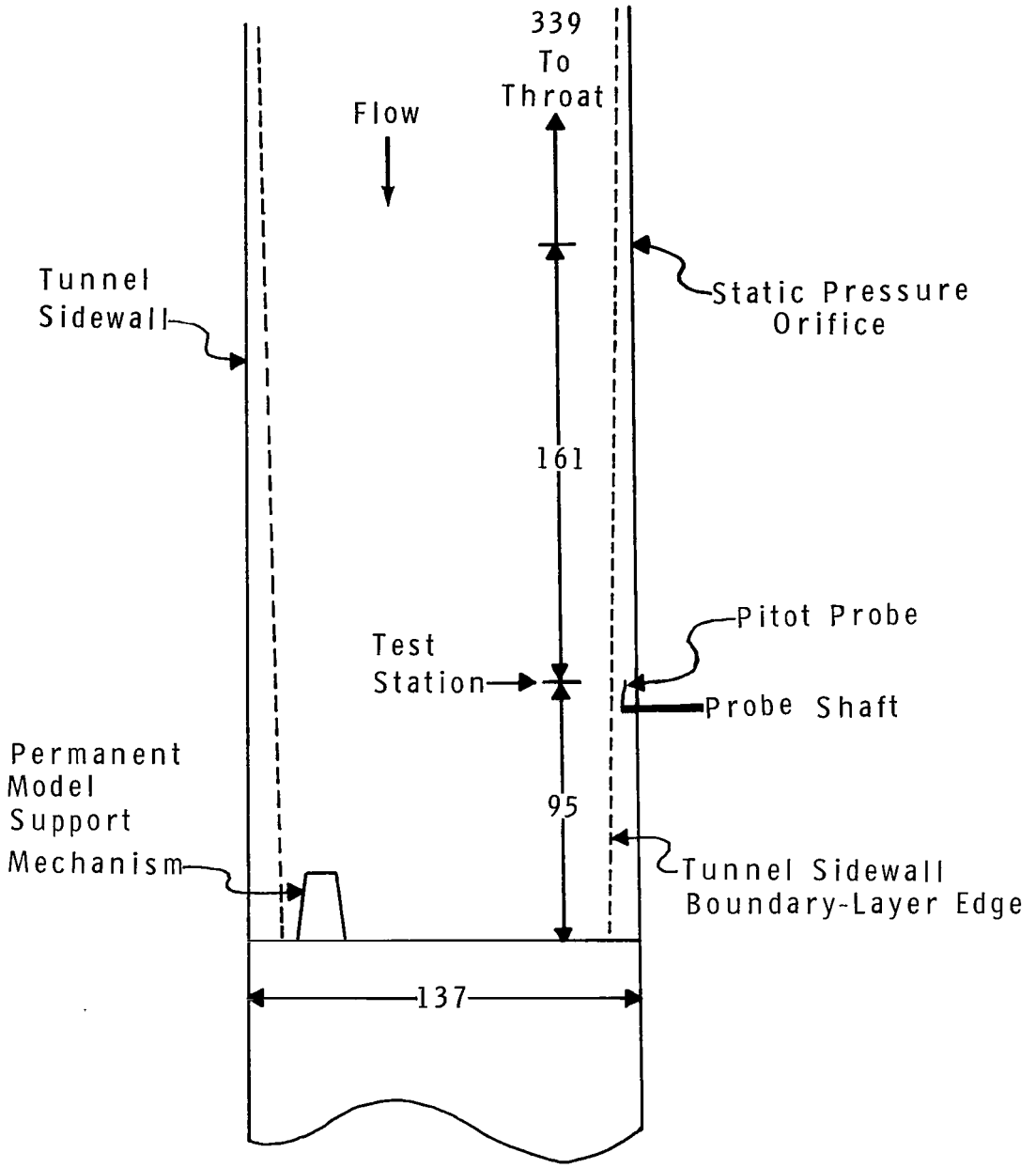

Figure 1.- Test-section sketch. All dimensions are in centimeters.

Circular Probes

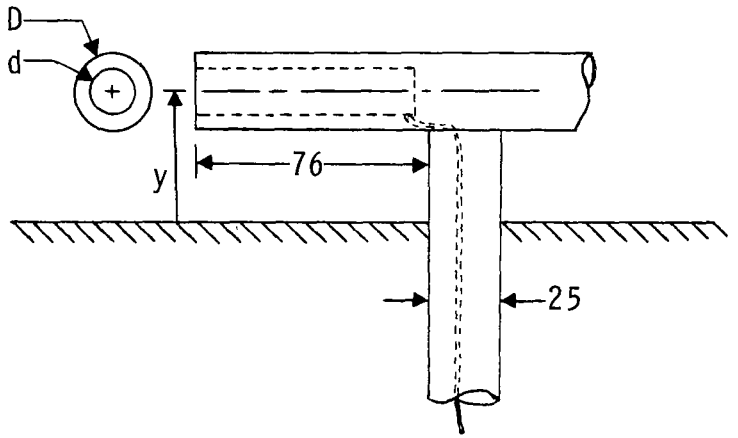

Flattened Reference Probe

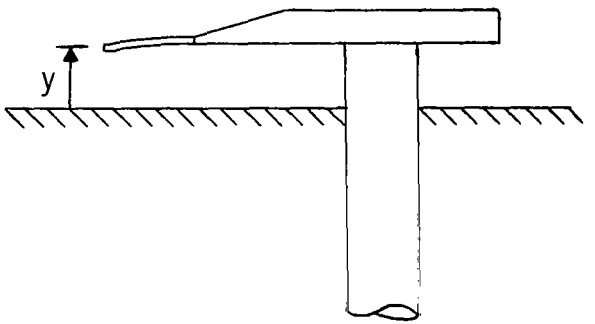

Probe Diameters

Probe	d	D	d/D
1	0.76	1.27	.60
2	1.40	2.38	.59
3	6.10	10.2	.60
4	10.7	17.8	.60
5	15.2	25.4	.60
6	19.8	33.0	.60
7	24.4	40.6	.60
8	29.0	48.3	.60

Probe Tip

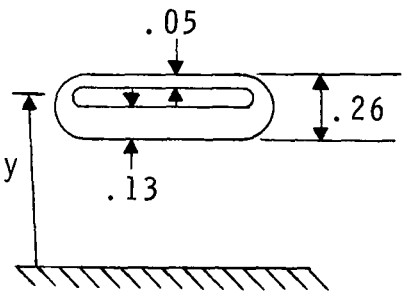

Figure 2.- Probe sketches. All dimensions are in millimeters.

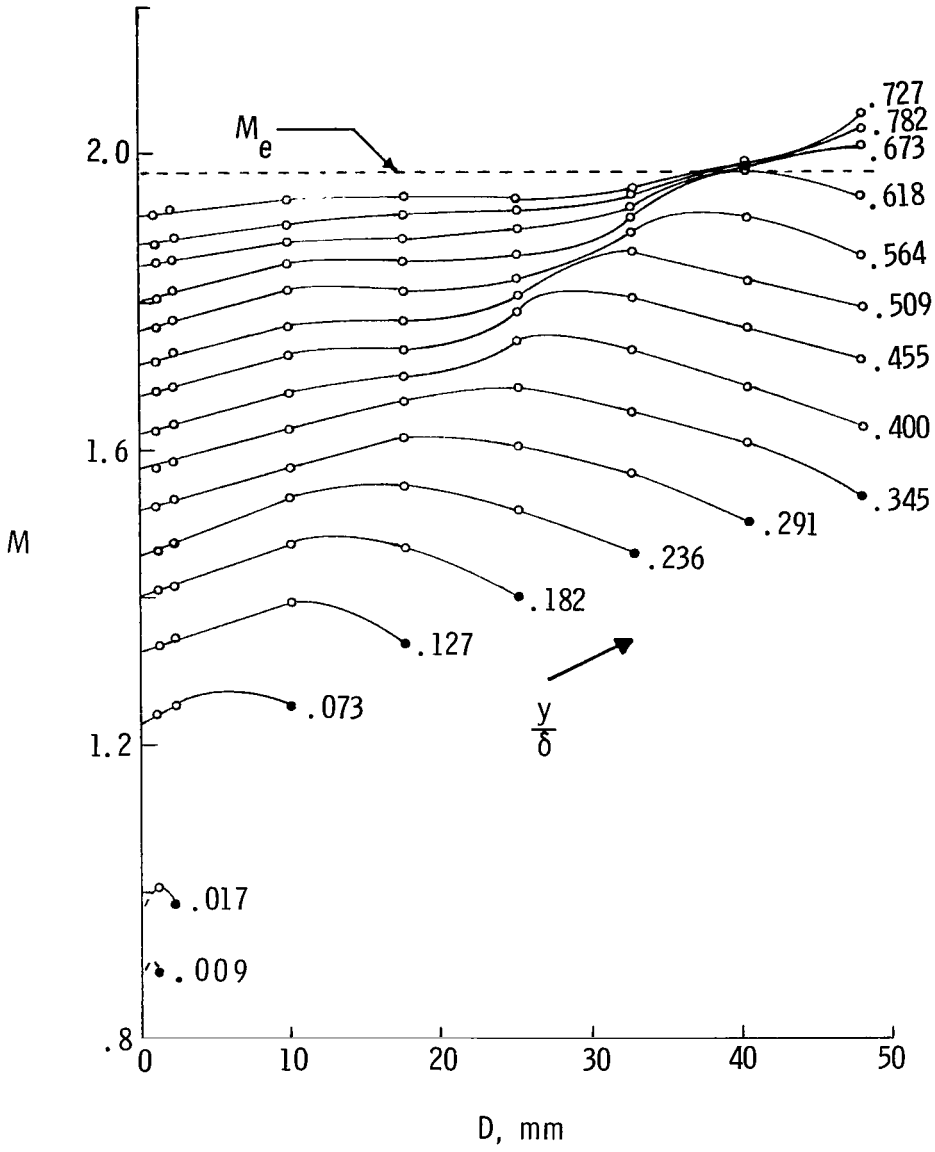

Figure 3.- Effect of probe size on indicated Mach numbers. Solid symbols denote data obtained with probe touching tunnel wall.

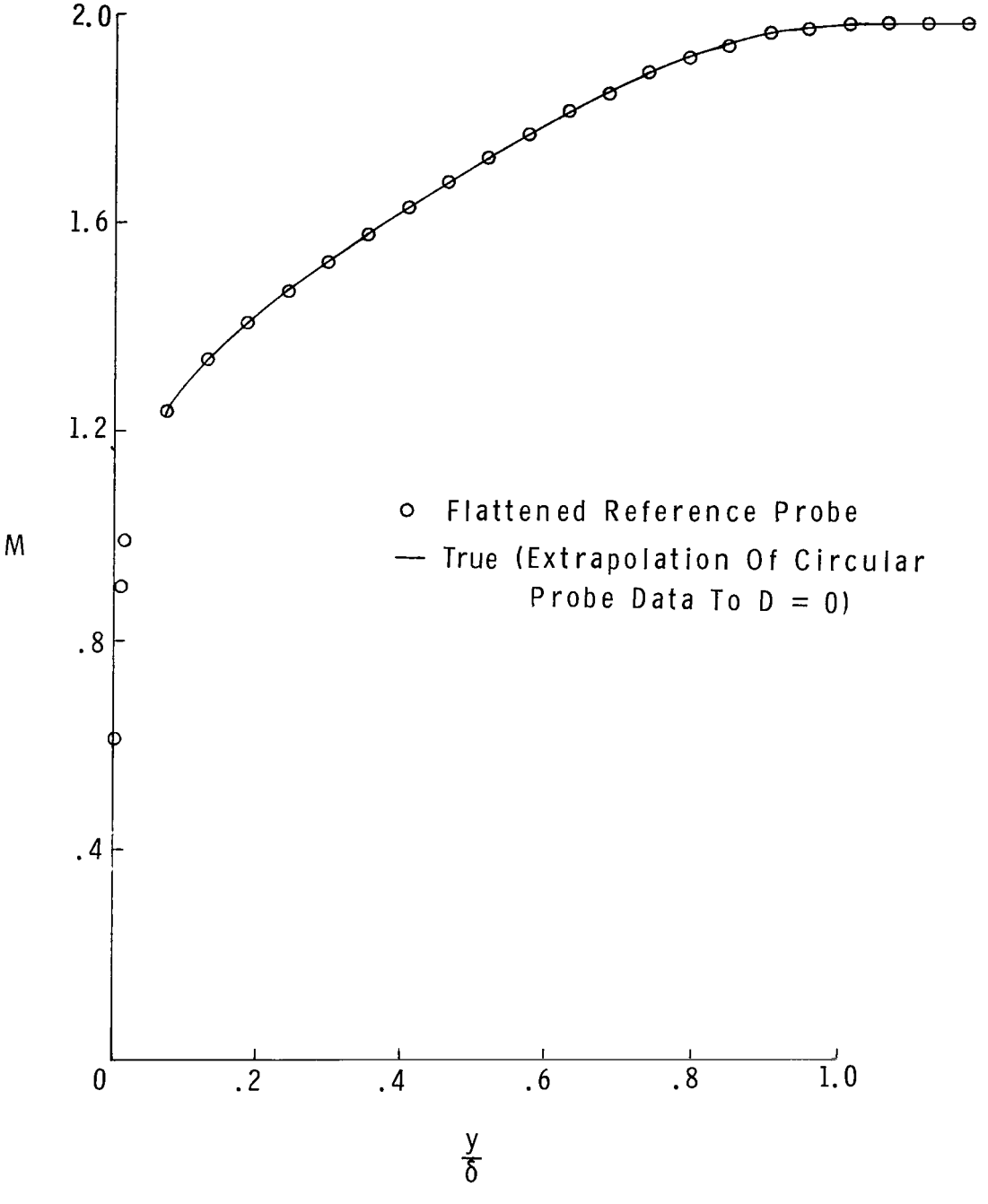

Figure 4.- Comparison of true and flattened-reference-probe profiles.

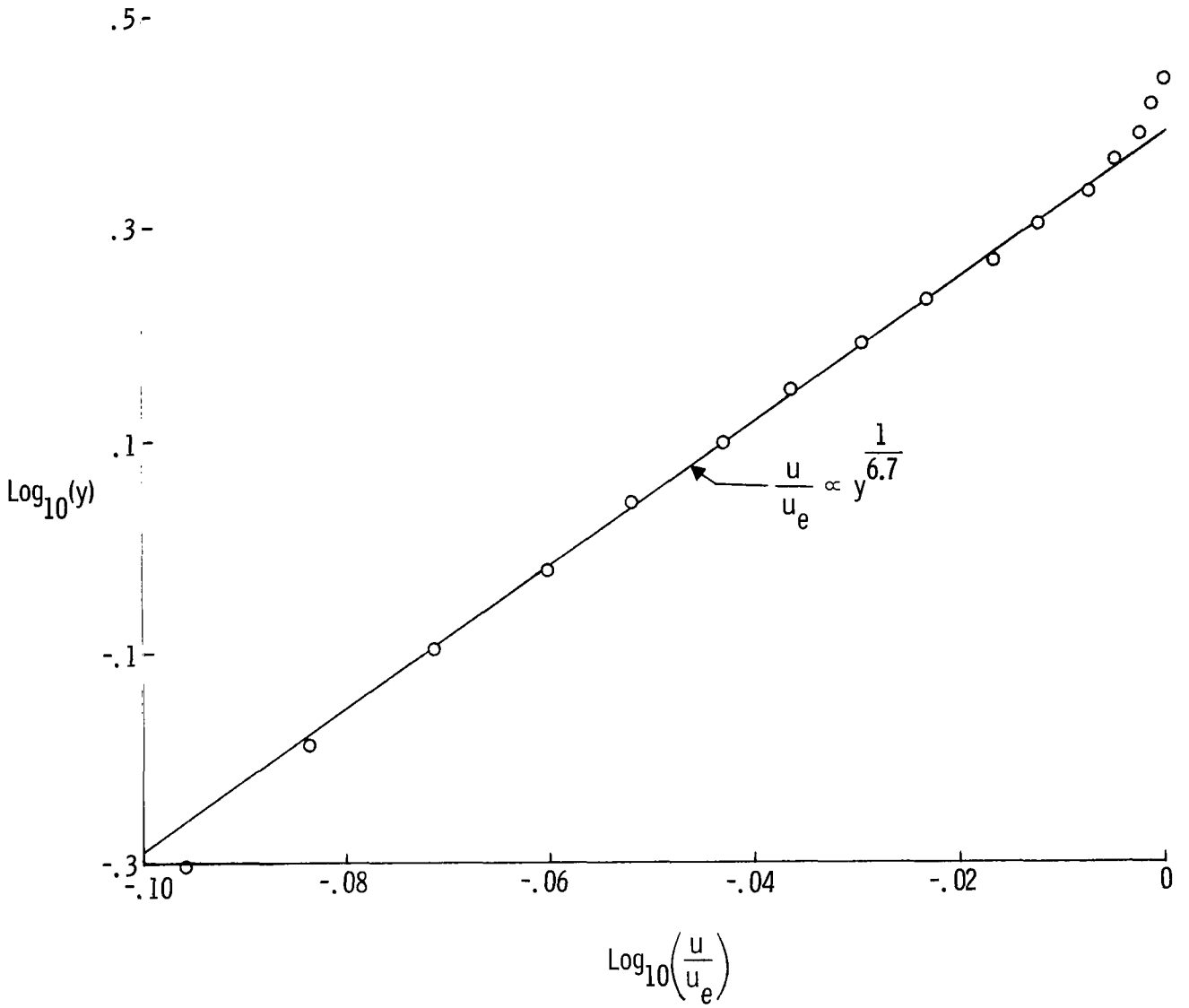

Figure 5.- True velocity profile in log-log form.

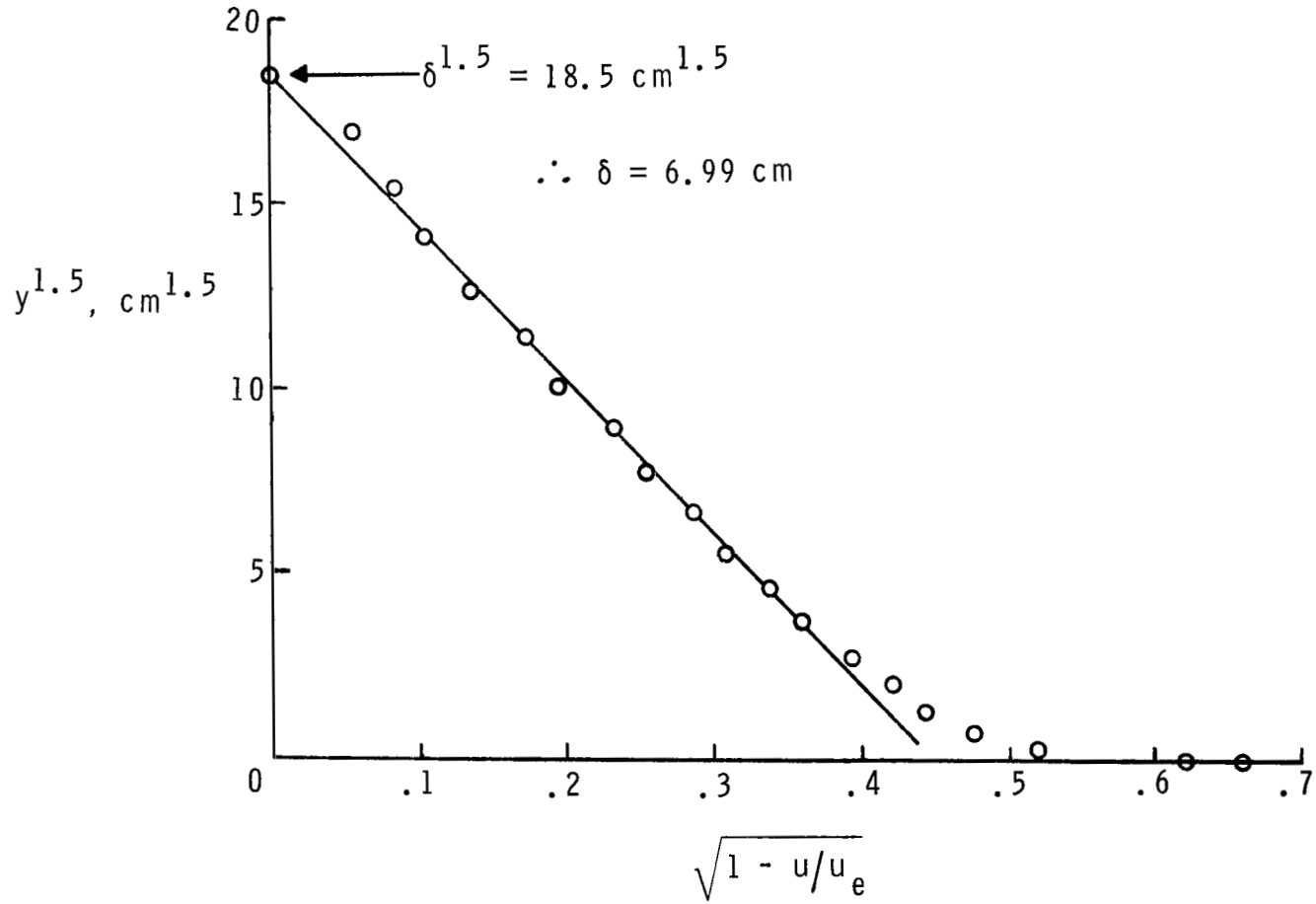

Figure 6.- Estimation of boundary-layer thickness.

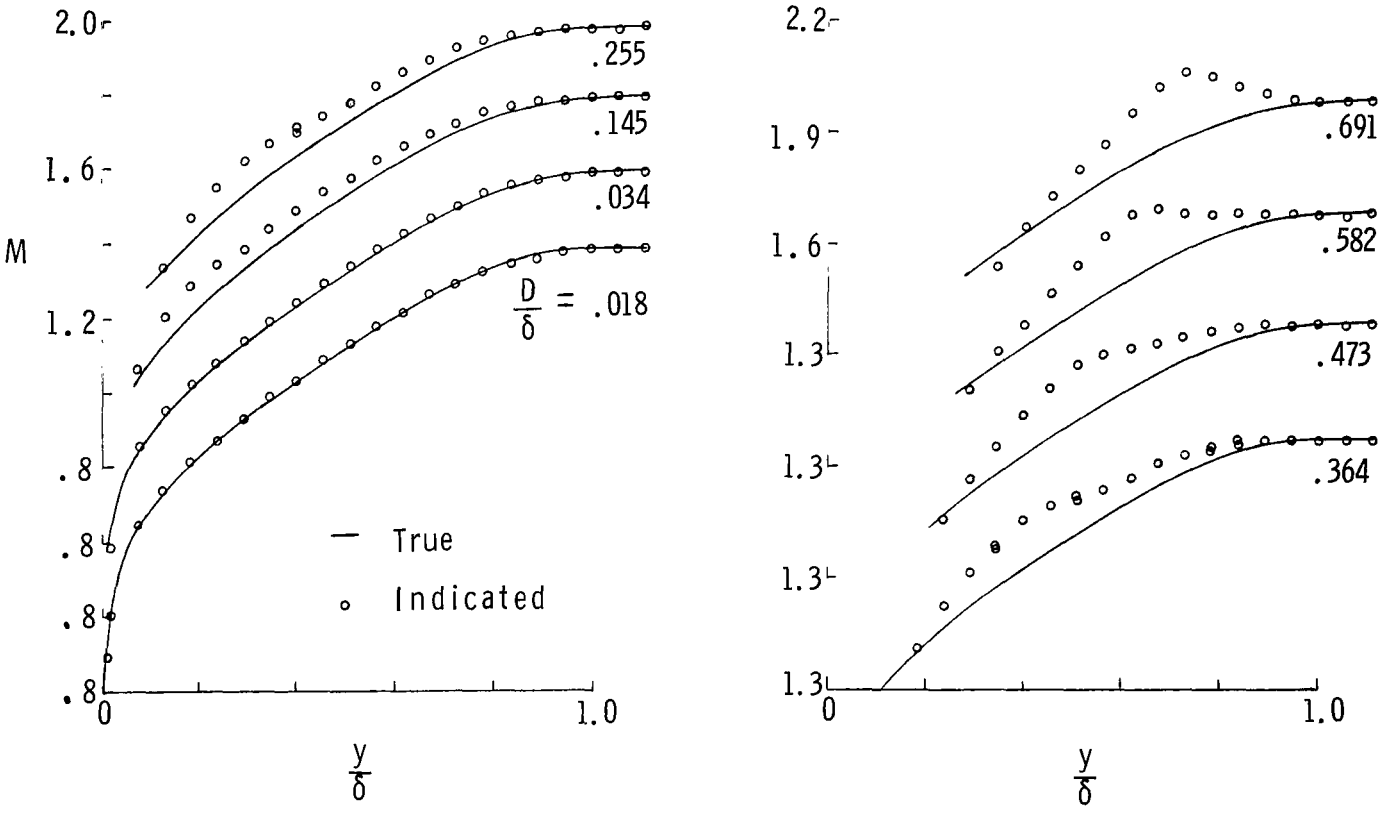

Figure 7.- Comparison of true and indicated profiles.

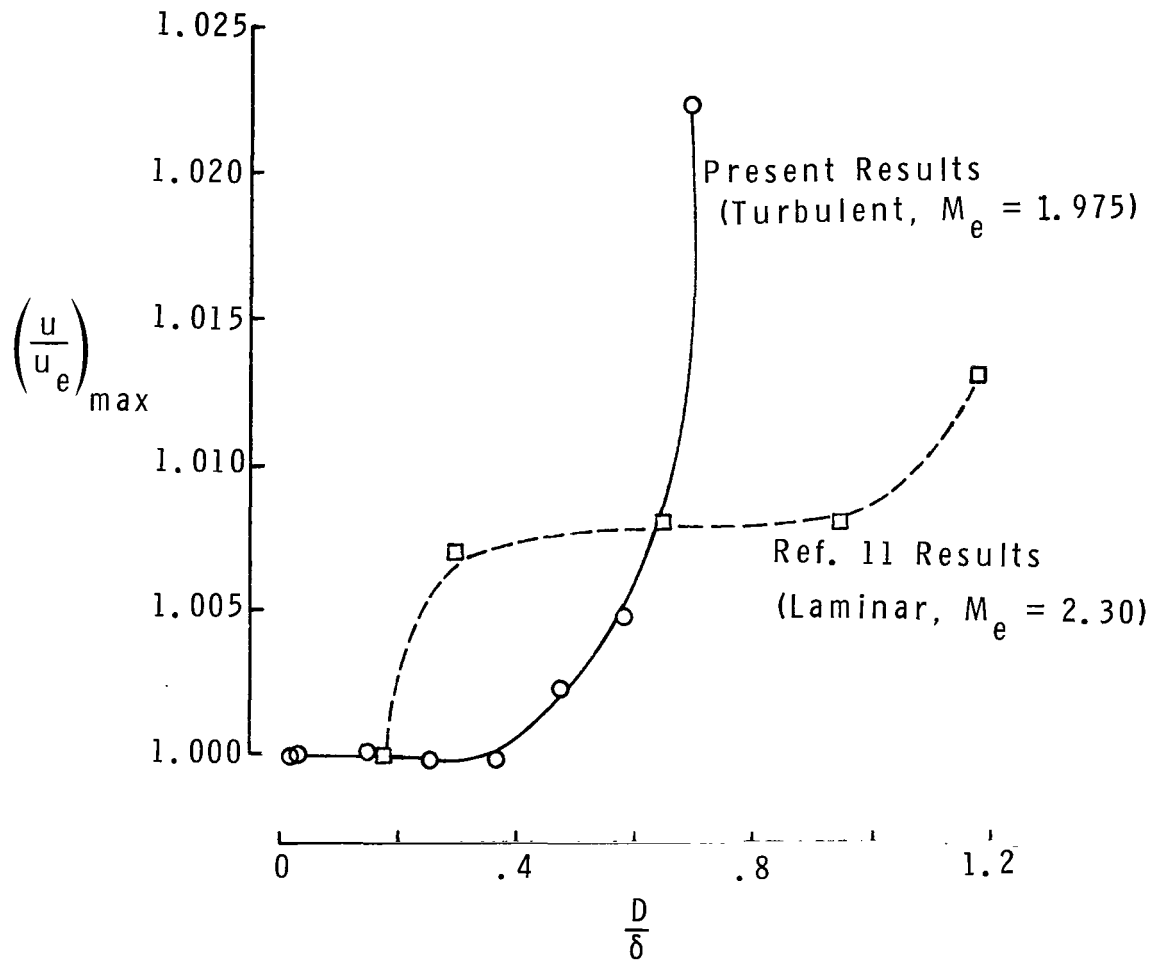

Figure 8.- Comparison of overshoot in laminar and turbulent boundary layers.

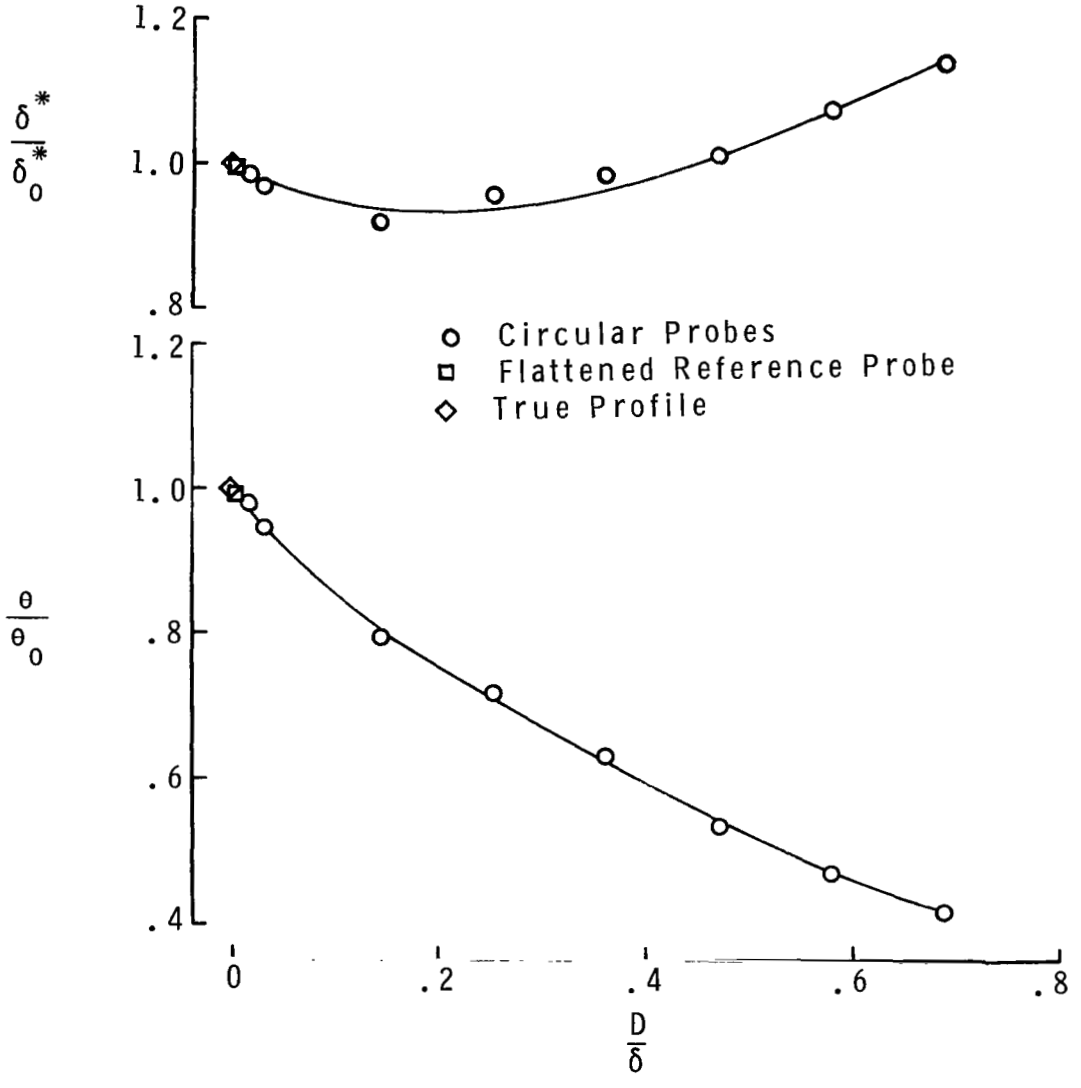

Figure 9.- Effect of probe size on experimental integral thicknesses.

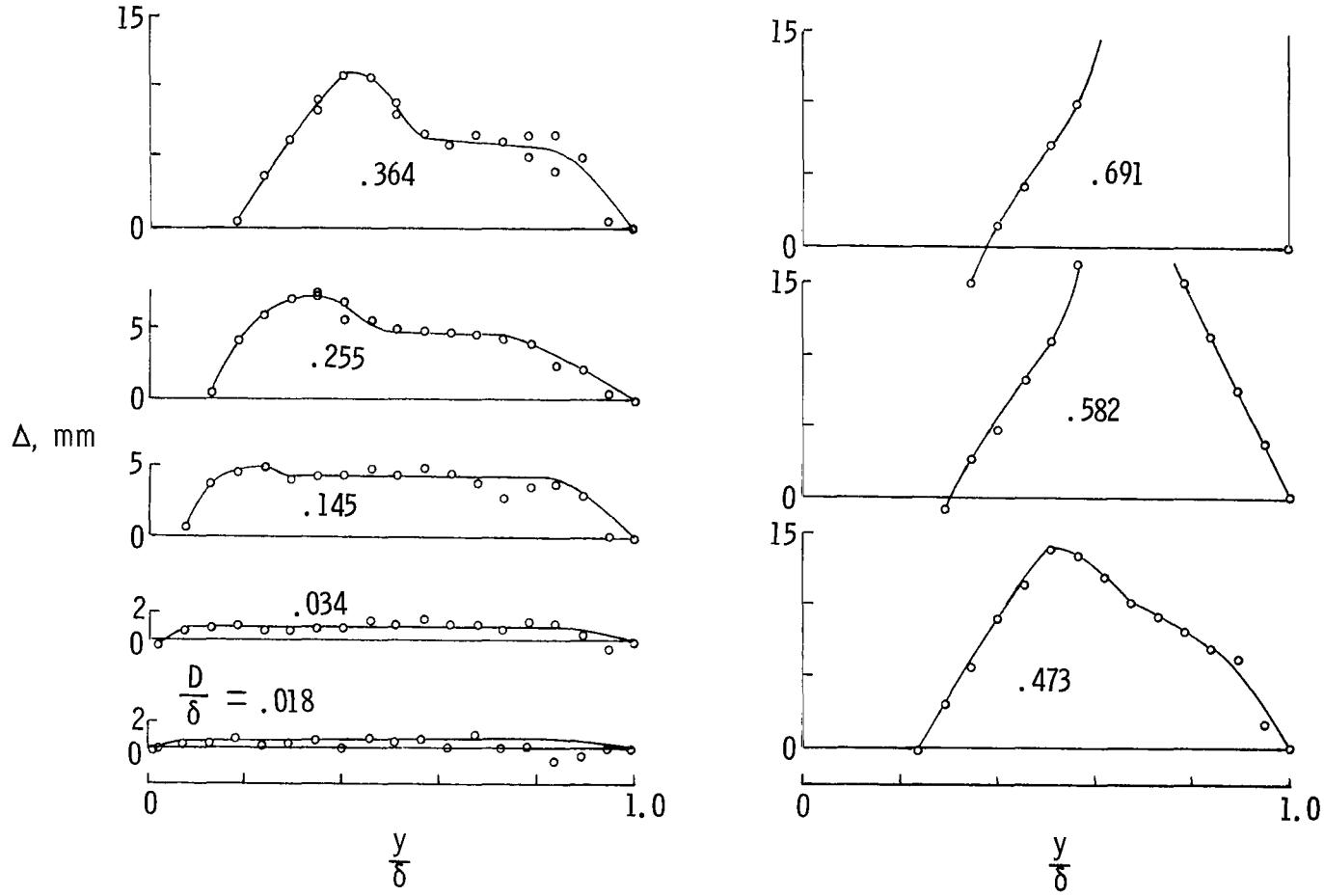

Figure 10.- Pitot-probe displacement distributions.

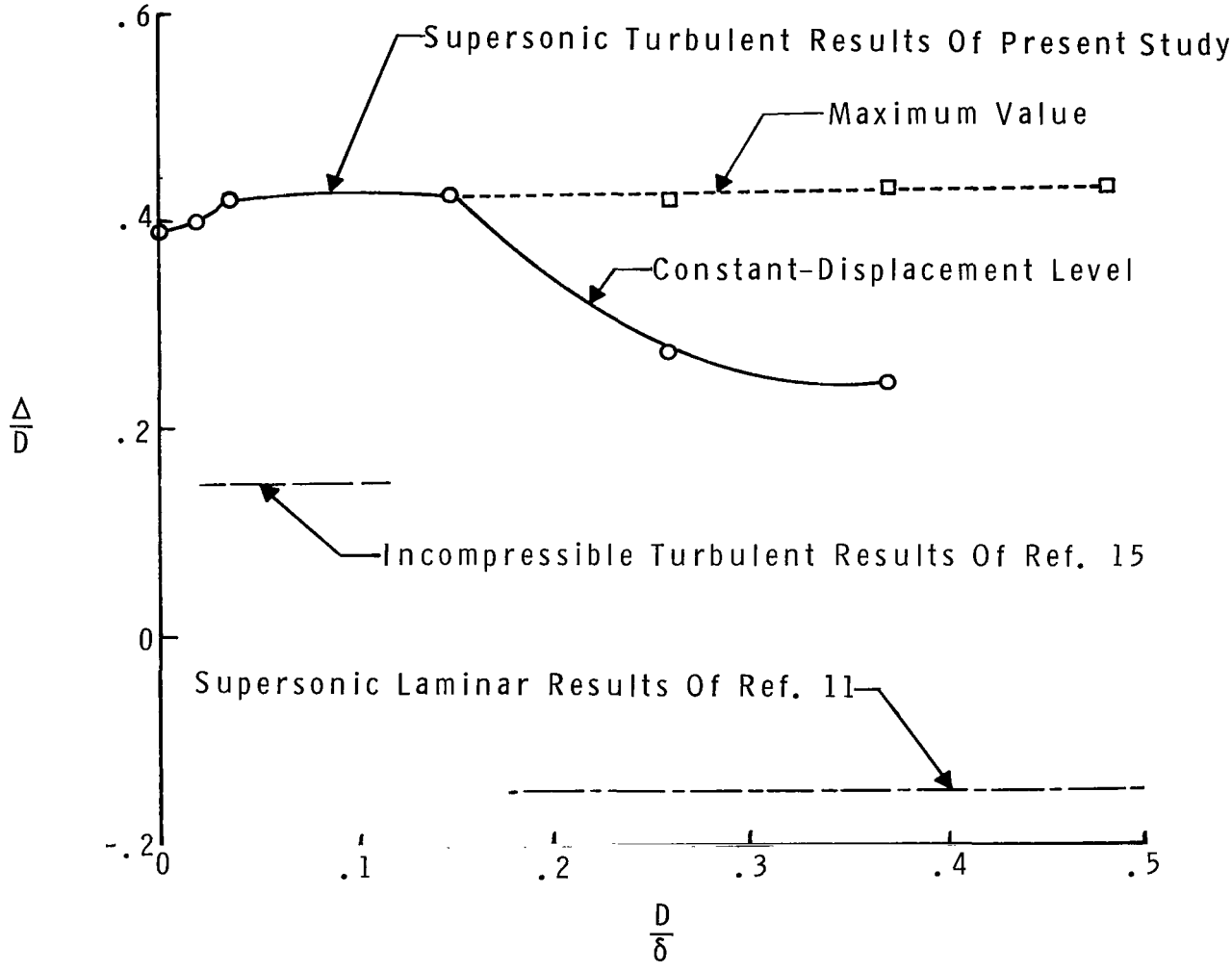

Figure 11.- Effect of probe size on displacement ratio in boundary layers.

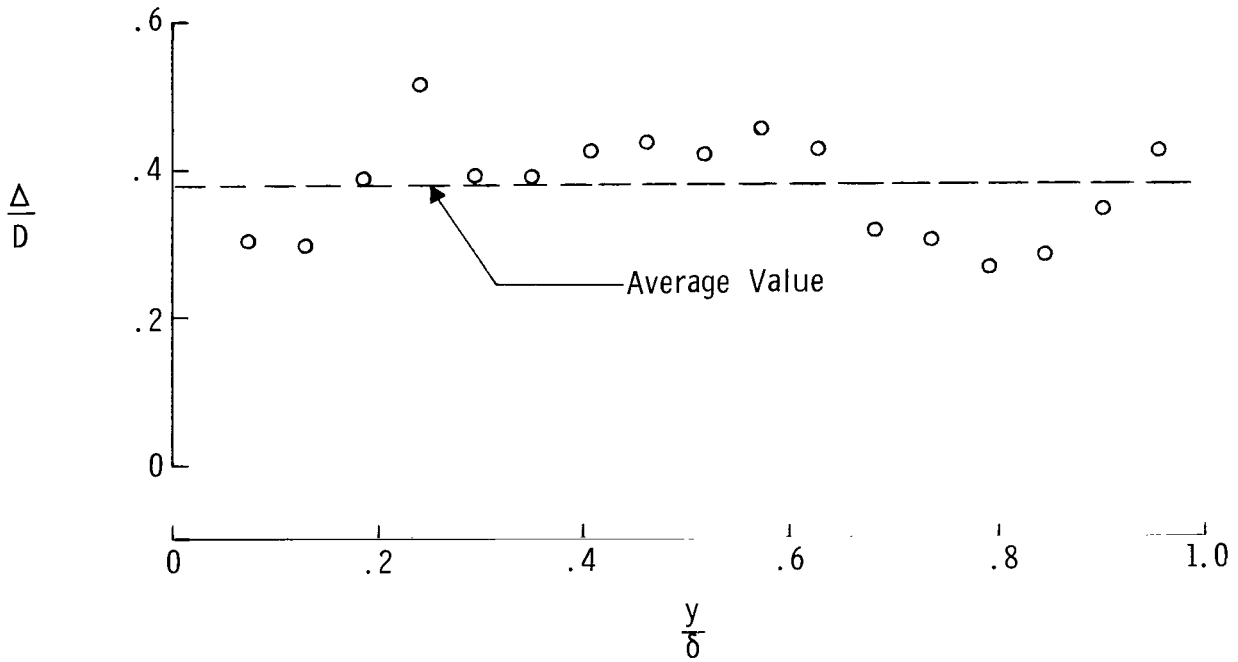

Figure 12.- Displacement distribution at zero diameter.

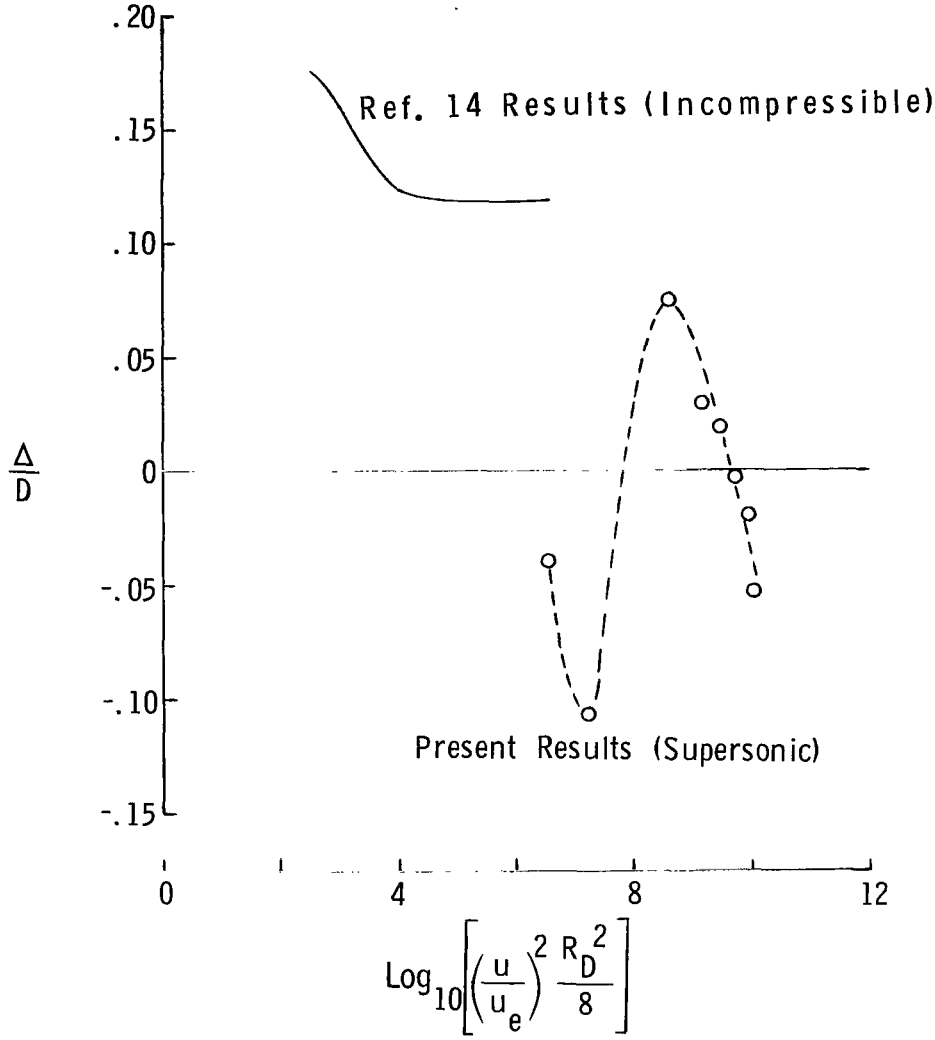

Figure 13.- Displacement ratio for probes in contact with wall.

"The aeronautical and space activities of the United States shall be conducted so as to contribute . . . to the expansion of human knowledge of phenomena in the atmosphere and space. The Administration shall provide for the widest practicable and appropriate dissemination of information concerning its activities and the results thereof."

—NATIONAL AERONAUTICS AND SPACE ACT OF 1958

NASA SCIENTIFIC AND TECHNICAL PUBLICATIONS

TECHNICAL REPORTS: Scientific and technical information considered important, complete, and a lasting contribution to existing knowledge.

TECHNICAL NOTES: Information less broad in scope but nevertheless of importance as a contribution to existing knowledge.

TECHNICAL MEMORANDUMS: Information receiving limited distribution because of preliminary data, security classification, or other reasons.

CONTRACTOR REPORTS: Scientific and technical information generated under a NASA contract or grant and considered an important contribution to existing knowledge.

TECHNICAL TRANSLATIONS: Information published in a foreign language considered to merit NASA distribution in English.

SPECIAL PUBLICATIONS: Information derived from or of value to NASA activities. Publications include conference proceedings, monographs, data compilations, handbooks, sourcebooks, and special bibliographies.

TECHNOLOGY UTILIZATION PUBLICATIONS: Information on technology used by NASA that may be of particular interest in commercial and other non-aerospace applications. Publications include Tech Briefs, Technology Utilization Reports and Technology Surveys.

Details on the availability of these publications may be obtained from:

SCIENTIFIC AND TECHNICAL INFORMATION OFFICE

NATIONAL AERONAUTICS AND SPACE ADMINISTRATION

Washington, D.C. 20546